Characterization of Mercury(II) Complexes of Bis[(2-pyridyl)methyl]amine by X-ray Crystallography and NMR Spectroscopy

Deborah C. Bebout,* Anne E. DeLanoy, and David E. Ehmann

Chemistry Department, The College of William and Mary, Williamsburg, Virginia 23187

Margaret E. Kastner and Damon A. Parrish

Chemistry Department, Bucknell University, Lewisburg, Pennsylvania 17837

Raymond J. Butcher

Chemistry Department, Howard University, Washington, D.C. 20059

Received November 26, 1997

Solution-state NMR and X-ray crystallography were used to investigate the complexation of Hg(II) by the tridentate ligand bis[(2-pyridyl)methyl]amine (BMPA). Mercury coordination compounds exhibiting rarely observed solution-state NMR $^{1}H^{199}Hg$ satellites were characterized. Temperature and concentration effects on solution-state NMR properties were investigated. The solution-state NMR were correlated with two solid-state structures. The distorted trigonal prismatic complex $[Hg(BMPA)_2](ClO_4)_2 \cdot 0.5$toluene (**1**) crystallizes in the triclinic space group $P\bar{1}$ with $a = 10.953(5)$ Å, $b = 12.812(5)$ Å, $c = 13.006(5)$ Å, $\alpha = 67.50(3)°$, $\beta = 82.74(3)°$, $\gamma = 67.88(3)°$, and $Z = 2$. The $Hg-N_{amine}$ bonds are 2.404(4) and 2.350(4) Å and the $Hg-N_{pyridyl}$ bond lengths are similar, ranging from 2.352(4) to 2.557(5) Å. Solution NMR studies are consistent with rapid equilibrium between isomeric trigonal prismatic and facial octahedral forms of this complex. A twisting mechanism is proposed to mediate interconversion. The distorted square planar complex $[Hg(BMPA)NCCH_3](ClO_4)_2$ (**7**) crystallizes in the monoclinic space group $P2_1/c$ with $a = 12.987(2)$ Å, $b = 17.469(4)$ Å, $c = 8.886(2)$ Å, $\beta = 95.200(12)°$, and $Z = 4$. The $Hg-N_{amine}$ distance is 2.403 Å, the average $Hg-N_{pyridyl}$ distance is 2.23 Å, and the $Hg-N_{nitrile}$ distance is 2.229 Å. The BMPA ligand is bound to Hg(II) in a meridional fashion with a solvent molecule in the same plane and close associations to two axial perchlorates with Hg−O distances of 2.707(7) and 2.90(2) Å. Solution NMR studies support limited dynamics for a cation with similar interactions between BMPA and Hg(II).

Introduction

Interest in development of ^{199}Hg nuclear magnetic resonance (NMR) as a metallobioprobe is increasing due to recent Hg(II) substitution into native copper,[1] zinc,[2] and iron[3] metal-binding protein sites with preservation of the coordination sphere of the metal and minimal changes in overall protein structure. Evidence for new classes of metal-binding motifs in enzymes, transcription factors, and regulatory proteins underscores the need for structural insights about local metal coordination environments.[4] Additional ^{199}Hg NMR structure−spectroscopy correlations would complement existing correlations for ^{113}Cd NMR. The latter have proven to be particularly useful for structural elucidation of Zn(II)- and Ca(II)-proteins.[5] Potential advantages of using Hg(II) for protein substitution studies include the larger chemical shift dispersion, shorter relaxation times, strong bonds formed between Hg(II) and N- and S-donors, and accessibility of one-electron redox chemistry.

Mercury has two NMR-active isotopes: ^{199}Hg and ^{201}Hg. ^{201}Hg is quadrupolar, leading to excessive line broadening that precludes routine observation. However, ^{199}Hg has $I = {}^1/_2$, 16.8% natural abundance and a receptivity 5.4 times that of ^{13}C. Heteronuclear coupling constants for ^{199}Hg in alkylmercurials[6] have been determined to increase in the order $^1J \gg {}^3J > {}^2J > {}^4J$. At this time, however, few coupling constant data for small nitrogen coordination compounds of mercury are available.[7]

(1) (a) Church, W. B.; Guss, J. M.; Freeman, H. C. *J. Biol. Chem.* **1986**, *261*, 234. (b) Utschig, L. M.; Wright, J. G.; Dieckmann, G.; Pecoraro, V.; O'Halloran, T. V. *Inorg. Chem.* **1995**, *34*, 2497.
(2) (a) Marmorstein, R.; Carey, M.; Ptashne, M.; Harrison, S. C. *Nature* **1992**, *356*, 408. (b) Cass, A. E. G.; Galdes, A.; Hill, H. A. O.; McClelland, C. E.; Storm, C. B. *FEBS Lett.* **1978**, *94*, 311.
(3) Blake, P. R.; Lee, B.; Summers, M. F.; Park, J.-B.; Zhou, Z. H.; Adams, M. W. W. *New J. Chem.* **1994**, *18*, 387.
(4) (a) Karlin, K. D. *Science* **1993**, *261*, 701. (b) O'Halloran, T. V. *Science* **1993**, *261*, 715. (c) Lippard, S. J.; Berg, J. M. *Principles of Bioinorganic Chemistry*; University Science: Mill Valley, CA, 1994. (d) Schwabe, J. W. R.; Klug, A. *Nature Struct. Biol.* **1994**, *1*, 345.
(5) Summers, M. F. *Coord. Chem. Rev.* **1988**, *86*, 43.
(6) (a) Wrackmeyer, B.; Contreres, R. *Annu. Rep. NMR Spectrosc.* **1992**, *24*, 267. (b) Granger, P. In *Transition Metal Nuclear Magnetic Resonance*; Pregosin, P. S., Ed.; Elsevier: New York, 1991; p 306.
(7) (a) Schlager, O.; Wieghardt, K.; Grondey, H.; Rufínska, A.; Nuber, B. *Inorg. Chem.* **1995**, *34*, 6440. (b) Bashall, A.; McPartlin, M.; Murphy, B. P.; Powell, H. R.; Waikar, S. *J. Chem. Soc., Dalton Trans.* **1994**, 1383. (c) McWhinnie, W. R.; Monsef-Mirzai, Z.; Perry, M. C.; Shaikh, N.; Hamor, T. A. *Polyhedron* **1993**, *12*, 1193. (d) Nivorozhkin, A. L.; Sukholenko, E. V.; Nivorozhkin, L. E.; Borisenko, N. I.; Minkin, V. I. *Polyhedron* **1989**, *8*, 569. (e) McCrindle, R.; Ferguson, G.; McAlees, A. J.; Parvez, M.; Ruhl, B. L.; Stephenson, D. K.; Wieckowski, T. *J. Chem. Soc., Dalton Trans.* **1986**, 2351.

S0020-1669(97)01499-7 CCC: $15.00
Published on Web 06/15/1998

We recently reported solution- and solid-state characterization of the mercury coordination chemistry of the potentially tetradentate ligand tris[(2-pyridyl)methyl]amine (TMPA).[8] This and related ligands are commonly used to provide synthetic models of protein metal-binding sites. We were able to detect cations of stoichiometry $[Hg(TMPA)_2]^{2+}$, $[Hg(TMPA)]^{2+}$, and $[Hg(TMPA)Cl]^{+}$ which were exchange-inert on the NMR time scale in acetonitrile at 20 °C. The three-bond coupling constants detected were similar in magnitude to those observed for the δ- and ϵ-protons of histidine in Hg(II)-substituted proteins.[2b,9]

As an extension of this work, we have investigated the mercury coordination chemistry of the related potentially tridentate ligand bis[(2-pyridyl)methyl]amine (BMPA, **8**). This

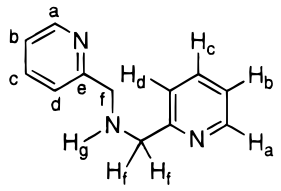

8

ligand has been used directly, and as part of higher coordinate ligand systems, to construct metal complexes modeling the spectroscopic or chemical properties of a wide variety of protein metal-binding sites. Crystallographic characterization of BMPA metal complexes has revealed bidentate[10,11] and both facial[10,12,13] and meridional[11,14] tridentate coordination geometries for BMPA. To the best of our knowledge, previous studies of BMPA with Hg(II) are limited to potentiometry[15] and IR.[16]

X-ray crystallographic structures are reported here for $[Hg(BMPA)_2](ClO_4)_2 \cdot 0.5$ toluene (**1**) and $[Hg(BMPA)NCCH_3](ClO_4)_2$ (**7**). The solution equilibria of $Hg(ClO_4)_2$ with BMPA in acetonitrile are analyzed in the context of these structures.

Experimental Section

Methods and Materials. Bis[(2-pyridyl)methyl]amine was obtained from TCI, America, and all other chemicals were obtained as reagent grade from Aldrich or Fisher. FT-IR spectra were recorded in KBr pellets on a Perkin-Elmer 1600. Elemental analyses were carried out by Atlantic Microlab, Inc., Norcross, GA.

Table 1. Selected Crystallographic Data

	$[Hg(BMPA)_2](ClO_4)_2 \cdot 0.5C_7H_8$ (**1**)	$[Hg(BMPA)NCCH_3](ClO_4)_2$ (**7**)
empirical formula	$C_{27.5}H_{30}N_6O_8Cl_2Hg$	$C_{14}H_{16}N_4O_8Cl_2Hg$
fw	844.07	639.80
space group	triclinic, $P\bar{1}$ (No. 2)	monoclinic, $P2_1/c$ (No. 14)
a, Å	10.953(5)	12.987(2)
b, Å	12.812(5)	17.469(4)
c, Å	13.006(5)	8.886(2)
α, deg	67.50(3)	90
β, deg	82.74(3)	95.200(12)
γ, deg	67.88(3)	90
V, Å^3	1561.8(11)	2007.8(7)
Z	2	4
d_{calc}, g/cm^3	1.795	2.117
μ, cm^{-1}	51.57	79.82
radiation (monochromatic)	Mo Kα ($\lambda = 0.710\ 73$ Å)	Mo Kα ($\lambda = 0.710\ 73$ Å)
T, °C	21	21
R1[a]	0.0452	0.0972
R2[b]	0.1019	0.1566

[a] $R1 = \sum||F_o| - |F_c||/\sum|F_o|$. [b] $R2 = \{\sum[w(F_o^2 - F_c^2)^2]/\sum[w(F_o^2)^2]\}^{1/2}$.

All of the perchlorate salts of mercury(II) complexes included in this work were stable for routine synthesis and purification procedures. However, caution should be exercised because perchlorate salts of metal complexes with organic ligands are potentially explosive.[17]

Synthesis of the Complex $[Hg(BMPA)_2](ClO_4)_2 \cdot 0.5$toluene (1). A solution of $Hg(ClO_4)_2 \cdot 3H_2O$ (0.45 g, 1.0 mmol) in 5.5 mL of acetonitrile was added to a solution of freshly distilled BMPA (0.46 g, 2.5 mmol) in acetonitrile (5.5 mL) with stirring. This solution was diluted 1:1 with toluene and set aside for slow evaporation. Colorless plates formed in 2 days. Mp: 175−178 °C. ^{1}H NMR (2 mM, CD_3CN, −40 °C): δ 7.99 (dd, 4 H, $J = 7$, 8 Hz, H_c), 7.85 (d, 4 H, $J = 4$ Hz, H_a), 7.55 (d, 4 H, $J = 7$ Hz, H_d), 7.38 (dd, 4 H, $J = 2$, 8 Hz, H_b), 7.28−7.09 (m, 2.5 H, toluene), 4.35 (b s, 4 H, H_f), 3.99 (b s, 4 H, $H_{f'}$). IR (KBr, cm^{-1}, Figure S9 (Supporting Information)): 3065 w, 3014 w, pyridine C−H; 1589 s, py C═N; 1477 s, 1441 s, 1431 s, pyridine C═C; 1143 vs, 1112 vs, 1081 vs, ClO_4; 1568 m; 1281 m; 1046 m; 1012 s; 994 m; 853 m; 774 s; 761 s; 635 s; 628 s. Anal. Calc for $C_{27.5}H_{30}Cl_2HgN_6O_8$: C, 39.14; H, 3.58; N, 9.96. Found: C, 39.34; H, 3.63; N, 9.94.

Synthesis of the Complex $[Hg(BMPA)NCCH_3](ClO_4)_2$ (7). A solution of freshly distilled BMPA (0.24 g, 1.2 mmol) in acetonitrile (2.5 mL) was added to an acetonitrile solution (2.5 mL) of $Hg(ClO_4)_2 \cdot 3H_2O$ (0.48 g, 1.2 mmol) with stirring. Toluene (5 mL) was added slowly with stirring, and the solution was set aside for slow evaporation. Colorless crystals of the complex suitable for X-ray crystallography formed upon standing for 3 days. The crystals turned white upon heating to 150 °C and melted with decomposition at 203−204 °C. ^{1}H NMR (2 mM, CD_3CN, 20 °C): δ 8.62 (d, 2 H, ^3J(HHg) = 46 Hz, $J = 5$ Hz, H_a), 8.12 (dt, 2 H, $J = 2$, 7 Hz, H_c), 7.70 (t, 2 H, $J = 6$ Hz, H_b), 7.60 (d, 2 H, ^3J(HHg) = 24 Hz, $J = 8$ Hz, H_d), 4.51 (dd, 2 H, ^3J(HHg) = 80 Hz, $J = 6$, 16 Hz, H_f), 3.92 (dd, 2 H, ^3J(HHg) = 41 Hz, $J = 7$, 15 Hz, $H_{f'}$), 2.12 (d, 2 H, $J = 6$ Hz, H_g). IR (KBr, cm^{-1}, Figure S10 (Supporting Information)): 1602 m, pyridine C═N; 1482 m, 1440 m, pyridine C═C; 1142 vs, 1113 vs, 1090 vs, ClO_4; 773 m; 626 m. Anal. Calc for $C_{14}H_{16}Cl_2HgN_5O_8$: C, 26.30; H, 2.52; N, 8.76. Found: C, 25.89; H, 2.51; N, 8.42.

X-ray Crystallography. Selected crystallographic data are given in Table 1, selected bond distances in Table 2, and selected bond angles in Table 3. Thermal ellipsoid plots are shown in Figures 1 and 2. Data were collected at 21 °C on a Siemens R3 (**1**) or P4S (**7**) four-circle diffractometer using graphite-monochromated Mo Kα X-radiation ($\lambda = 0.710\ 73$ Å) and the $\theta-2\theta$ technique over a 2θ range of 3−55°. The structures were solved by direct methods and Fourier

(8) Bebout, D. C.; Ehmann, D. E.; Trinidad, J. C.; Crahan, K. K.; Kastner, M. E.; Parrish, D. A. *Inorg. Chem.* **1997**, *36*, 4257.
(9) Utschig, L. M.; Bryson, J. W.; O'Halloran, T. W. *Science* **1995**, *268*, 380.
(10) Palaniandavar, M.; Butcher, R. J.; Addison, A. W. *Inorg. Chem.* **1996**, *35*, 467.
(11) Jenkins, H. A.; Yap, G. P. A.; Puddephatt, R. J. *Organometallics* **1997**, *16*, 1946.
(12) (a) Glerup, J.; Goodson, P. A.; Hodgson, D. J.; Michelsen, K.; Nielsen, K. M.; Weihe, H. *Inorg. Chem.* **1992**, *31*, 4611. (b) Butcher, R. J.; Addison, A. W. *Inorg. Chim. Acta* **1989**, *158*, 211.
(13) (a) Dick, S.; Weiss, A.; Wagner, U.; Wanger, F.; Grosse, G. *Z. Naturforsch.* **1997**, *52B*, 372. (b) Ama, T.; Okamoto, K.; Yonemura, T.; Kawaguchi, H.; Ogasawara, Y.; Yasui, T. *Chem. Lett.* **1997**, 29. (c) Brisdon, B. J.; Cartwright, M.; Hodson, A. G. W.; Mahon, M. F.; Molloy, K. C. *J. Organomet. Chem.* **1992**, *435*, 319. (d) O'Brien, R. J.; Richardson, J. F.; Buchanan, R. M. *Acta Crystallogr.* **1991**, *C47*, 2307. (e) Larsen, S.; Michelsen, K.; Pedersen, E. *Acta Chem. Scand.* **1986**, *A40*, 63.
(14) (a) Brand, U.; Burth, R.; Vahrenkamp, H. *Inorg. Chem.* **1996**, *35*, 1083. (b) Wirbser, J.; Vahrenkamp, H. *Z. Naturforsch.* **1992**, *47B*, 962. (c) Bang, E.; Michelsen, K.; Nielsen, K. M.; Pedersen, E. *Acta Chem. Scand.* **1989**, *43*, 748.
(15) Anderegg, G.; Hubmann, E.; Podder, N. G.; Wenk, F. *Helv. Chim. Acta* **1977**, *60*, 123.
(16) Madden, D. P.; da Mota, M. M.; Nelson, S. M. *J. Chem. Soc. A* **1970**, 790.
(17) (a) Wosley, W. C. *J. Chem. Educ.* **1973**, *50*, A335. (b) Raymond, K. N. *Chem. Eng. News* **1983**, *61*, (49), 4.

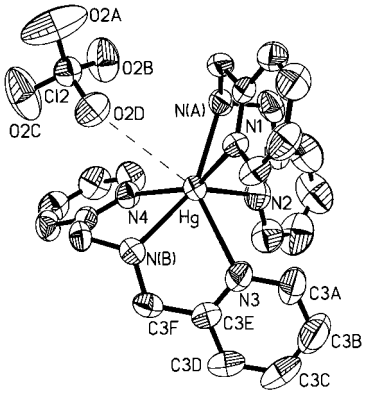

Figure 1. Thermal ellipsoid plot of the $[Hg(BMPA)_2](ClO_4)^+$ ion pair of **1**. Ellipsoids are at 50% probability. Hydrogens are omitted for clarity. Only one (2-pyridyl)methyl group has been completely labeled.

Table 2. Selected Bond Distances (Å) in $[Hg(BMPA)_2](ClO_4)_2 \cdot 0.5C_7H_8$ (**1**) and $[Hg(BMPA)NCCH_3](ClO_4)_2$ (**7**)

$[Hg(BMPA)_2](ClO_4)_2 \bullet 0.5\ C_7H_8$ (**1**)		$[Hg(BMPA)NCCH_3](ClO_4)_2$ (**7**)	
Hg−N(A)	2.404(4)	Hg−N	2.401(10)
Hg−N(B)	2.350(4)	Hg−N(1)	2.193(9)
Hg−N(1)	2.352(4)	Hg−N(2)	2.259(9)
Hg−N(2)	2.414(5)	Hg−N′	2.226(11)
Hg−N(3)	2.557(5)		
Hg−N(4)	2.418(4)		
$N-C(F)_{av}$	1.467(4)	$N-C(F)_{av}$	1.48(3)
$N-C(A)_{av}$	1.343(4)	$N-C(A)_{av}$	1.32(2)
$N-C(E)_{av}$	1.325(8)	$N-C(E)_{av}$	1.34(2)
$C(E)-C(F)_{av}$	1.501(9)	$C(E)-C(F)_{av}$	1.50(2)
		N′-C(1)	1.11(2)
		C(1)−C(2)	1.48(2)

Table 3. Selected Bond Angles (deg) in $[Hg(BMPA)_2](ClO_4)_2 \cdot 0.5C_7H_8$ (**1**) and $[Hg(BMPA)NCCH_3](ClO_4)_2$ (**7**)

$[Hg(BMPA)_2](ClO_4)_2 \bullet 0.5\ C_7H_8$ (**1**)		$[Hg(BMPA)NCCH_3](ClO_4)_2$ (**7**)	
N(A)−Hg−N(B)	153.1(2)	N−Hg−N′	155.8(4)
N(A)−Hg−N(1)	71.51(14)	N−Hg−N(1)	75.8(3)
N(B)−Hg−N(1)	108.06(13)	N−Hg−N(2)	74.4(4)
N(A)−Hg−N(2)	71.8(2)	N(1)−Hg−N(2)	135.5(3)
N(B)−Hg−N(2)	130.3(2)	N(1)−Hg−N′	117.6(4)
N(1)−Hg−N(2)	108.5(2)	N(2)−Hg−N′	102.7(4)
N(A)−Hg−N(3)	138.3(2)		
N(B)−Hg−N(3)	67.4(2)		
N(1)−Hg−N(3)	88.7(2)		
N(2)−Hg−N(3)	81.0(2)		
N(A)−Hg−N(4)	95.82(14)		
N(B)−Hg−N(4)	71.16(14)		
N(1)−Hg−N(4)	150.39(14)		
N(2)−Hg−N(4)	91.7(2)		
N(3)−Hg−N(4)	116.4(2)		
$Hg-N-C(E)_{av}$	114(3)	$Hg-N-C(E)_{av}$	116(2)
$Hg-N-C(F)_{av}$	109.5(14)	$Hg-N-C(F)_{av}$	106(2)
$Hg-N-C(A)_{av}$	125.3(5)	$Hg-N-C(A)_{av}$	123(2)
$C(A)-N-C(E)_{av}$	118.7(5)	$C(A)-N-C(E)_{av}$	120.2(9)

difference maps using the SHELXTL-PLUS[18] package of software programs. Final refinements were done using SHELXL-93[19] minimizing $R2 = [\sum[w(F_o^2) - (F_c^2)^2]/\sum[w(F_o^2)^2]^{1/2}$, $R1 = \sum||F_o| - |F_c||/\sum|F_o|$, and $S = [\sum[w(F_o^2 - F_c^2)^2]/(n - p)]^{1/2}$. All non-hydrogen atoms were refined as anisotropic, the hydrogen atomic positions were fixed relative to the bonded carbons, and the isotropic thermal parameters were refined.

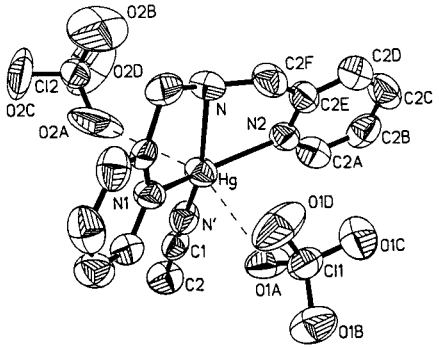

Figure 2. Thermal ellipsoid plot of $[Hg(BMPA)(NCCH_3)](ClO_4)_2$ (**7**). Ellipsoids are at 50% probability. Hydrogens are omitted for clarity. Only one (2-pyridyl)methyl group has been completely labeled, and only one of the two orientations of perchlorate (2) are shown.

X-ray Diffraction of $[Hg(BMPA)_2](ClO_4)_2 \cdot 0.5$ toluene (1). A cloudy, colorless plate measuring 0.50 × 0.26 × 0.13 mm was glued on the end of a glass fiber. During data collection, three standard reflections were measured after every 50 reflections. Although the crystal turned black in the beam, no decay of the intensity of the standard was observed and no absorption correction was performed on these data. The final data-to-parameter ratio was 17:1.

X-ray Diffraction of $[Hg(BMPA)NCCH_3](ClO_4)_2$ (7). A colorless plate measuring 0.32 × 0.48 × 0.42 mm was glued on the end of a glass fiber. During data collection, three standard reflections were measured after every 97 reflections. The crystal turned black in the beam. The intensity of the standards decreased about 10% during data collection, and all data were scaled on the basis of the standards. A partially disordered perchlorate was modeled by two sites with 0.49 occupancy for one and 0.51 occupancy for the other. The final data-to-parameter ratio was 12:1.

NMR Measurements. All solutions for NMR titration analysis were prepared by adding stock solutions of mercuric perchlorate in acetonitrile-d_3 to a solution of BMPA in acetonitrile-d_3 using calibrated autopipets. NMR spectra were recorded in 5-mm-o.d. NMR tubes on a General Electric QE-300 operating in the pulse Fourier transform mode. The sample temperature was maintained by blowing chilled air over the NMR tube in the probe. The variable-temperature unit was calibrated with methanol as previously described.[20] Chemical shifts were measured relative to internal solvent but are reported relative to tetramethylsilane.

Results

Crystal Structure of $[Hg(BMPA)_2](ClO_4)_2 \cdot 0.5$ toluene (1). The mercury ion is located at a general position with a distorted trigonal prism coordination sphere geometry. The tridentate ligands reduce the molecular symmetry to approximately C_2. Figure 1 shows the cation with one perchlorate anion. The molecular C_2 axis is nearly along the O(2D)−Hg axis. The pseudo-C_3 axis of the trigonal prismatic core is approximately perpendicular to the page. One triangular face consists of atoms N(A), N(2), and N(4), which eclipse the other triangular face of atoms N(1), N(3), and N(B), respectively. The $Hg-N_{amine}$ and $Hg-N_{pyridyl}$ bond distances are remarkably similar, except for the Hg−N(3) distance. Several differences between ring 3 and the other three rings were attributable to a packing effect. Figure S5 (Supporting Information) shows a crystallographic inversion center which orients rings 3 in two different molecules parallel at a separation of 3.7 Å. The Hg−N(3) distance, 2.557(5) Å, is 0.17 Å greater than the average of the other five Hg−N

(18) *SHELXTL-Plus*, Version 4.21/V.; Siemens Analytical X-ray Instruments, Inc.: Madison, WI, 1990.
(19) Sheldrick, G. M. In *Crystallographic Computing 6*; Flack, H. D., Parkanyi, L., Simon, K., Eds.; Oxford, U.K., 1993; p 111.
(20) Raiford, D. S.; Fisk, C. L.; Becker, E. D. *Anal. Chem.* **1979**, *51*, 2050.

distances, 2.39(4) Å. These distances are similar to the Hg−$N_{pyridyl}$ distances of 2.46(3) Å observed in the pseudooctahedral complex $[Hg(pyridine)_6](CF_3SO_3)_2$.[21] The five-membered chelating rings are each in an envelope conformation, with the methylene carbons, C_f, at the apex of the "flap" displaced by about 0.5 Å in rings 1, 2, and 4, but with the mercuric ion at the apex in ring 3, displaced by 1.2 Å.

An oxygen, O(2D), from one of the perchlorate anions is found along the pseudo-C_2 axis. The Hg−O(2D) distance of 3.35 Å is too long to be considered bonding. Other metal complexes of type $[M(BMPA)_2]$ with noncoordinating counterions possess very similar ligand geometry. These have been reported as having approximately octahedral metal-coordination geometry, most with required crystallographic symmetry C_i or C_2. The N−M−N angles reported for Mn(II), Cd(II), and one form of Zn(II)[12a] are very similar to those found for Hg(II). Additionally, the M−N_{amine} and M−$N_{pyridyl}$ distances are similar within each of these complexes. Particularly noteworthy are the $N_{pyridyl}$−M−$N_{pyridyl}$ bond angles which are in the range 108−117°. Each of these complexes would be better described as pseudo trigonal prisms rather than pseudooctahedrons. Whereas the Hg(II) complex has only molecular C_2 symmetry, the others have crystallographically required C_2 symmetry. Crystallographic C_2 symmetry is also found in the Fe(II)[12b] complex in which the $N_{pyridyl}$−Fe−$N_{pyridyl}$ bond angles are between 82 and 85°. This complex is well described as pseudooctahedral involving facial BMPA coordination with cis-N_{amines}. Among the complexes having C_2 symmetry, the octahedral Fe(II) complex is likely a ramification of the crystal field stabilization found in low-spin d^6 complexes but missing in the trigonal prismatic high-spin d^5 or d^{10} complexes of Mn(II), Cd(II), Zn(II), and Hg(II). Two other forms of $Zn(BMPA)_2^{2+}$ have been reported[12a] in which the metals are located at crystallographic inversion centers. One form of $Cu(BMPA)_2^{2+}$ has been reported with molecular C_i symmetry.[10] These C_i complexes have $N_{pyridyl}$−M−$N_{pyridyl}$ bond angles in the range 84−87° and can be described as pseudooctahedral involving facial BMPA coordination with trans-N_{amines}. The M−N bond distances reported for the Zn(II) complexes are nearly equal whereas in the Cu(II) complex a Jahn−Teller distortion results in two of the Cu−N pyridyl distances being significantly shorter than the other four Cu−N distances.

Crystal Structure of $[Hg(BMPA)NCCH_3](ClO_4)_2$ (7). The coordination sphere has approximate S_4 symmetry. The four nitrogen atoms, three from a BMPA ligand and one from acetonitrile, are displaced about 0.5 Å from their mean plane. As shown in Figure 2, one oxygen atom from each of the perchlorate anions is found along the vertical axis at librationally adjusted[22] distances of 2.707(7) Å (Hg−O(1A)) and 2.90(2) Å (Hg−O(2A), average of two sites with 0.49 occupancy for one and 0.51 occupancy for the other). The two five-membered chelate rings are in an "envelope" conformation, with the mercuric ion defining the apex of the "flap". The Hg−N_{amine} distance is approximately 0.18 Å longer than the other three Hg−N distances, which average 2.23(3) Å. The average Hg−$N_{pyridyl}$ distance is at the low end of the range previously reported for four-coordinate Hg(II) complexes involving ligation by pyridine derivatives.[23] The $N_{pyridyl}$−Hg−$N_{pyridyl}$ bond angle is 135°. This value is certainly larger than the ∼85° associated with facial coordination in octahedral systems and intermediate between the ∼115° found in trigonal prismatic structures and the ∼155° observed for nominally meridional coordination in the five-coordinate structures of Zn(II)[12a] and Cu(II).[10] Some implications of the wide range of $N_{pyridyl}$−Hg−$N_{pyridyl}$ bond angles will be amplified in the Discussion.

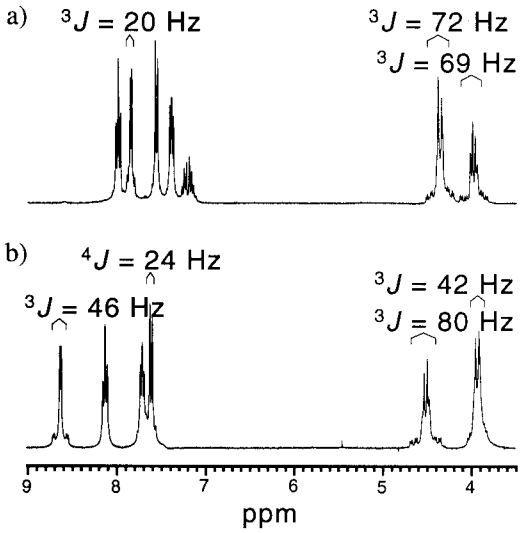

Figure 3. Proton NMR spectra recorded in CD_3CN for (a) 2 mM **1** at −40 °C with 4% excess $Hg(ClO_4)_2$ and (b) 2 mM **7** at 20 °C immediately after dissolving.

Investigation of BMPA Coordination of Hg(II) in the Solution State. Acetonitrile-d_3 solutions containing nominal molar ratios of BMPA and $Hg(ClO_4)_2$ were examined by ^1H NMR with total [Hg(II)] = 2−100 mM. Selected proton NMR spectra with 2 mM $Hg(ClO_4)_2$ are shown in Figure 3. The chemical shifts of the individual ^1H resonances as a function of [Hg(II)]/[BMPA] at 20 °C are shown in Figure 4.

Solutions containing 2 mM $Hg(ClO_4)_2$ had several notable features at 20 °C. In the presence of less than 0.5 equiv of $Hg(ClO_4)_2$, each of the symmetry-related protons of BMPA exhibited a single, sharp ^1H resonance. Two broad resonances for the methylene protons became apparent at 0.5 equiv. Between 0.5 and 0.75 equiv of Hg(II), the four pyridyl and two methylene proton resonances were severely broadened but nearly constant in apparent chemical shift. Additional broadened peaks for H_a and H_b and approximately linear drifts in the chemical shifts for other protons manifested the presence of another ligand environment between 0.75 and 1.0 equiv of $Hg(ClO_4)_2$. Sharp peaks with constant chemical shifts for four pyridyl proton environments and two methylene proton environments with a 15 Hz geminal splitting were observed with 1.0−2.0 equiv of Hg(II). Significantly, this set of resonances exhibited well-resolved $^3J(^1H^{199}Hg)$ of 46 and 80 Hz for H_a and one set of H_f, respectively. Additional satellites with $^3J(^1H^{199}Hg)$ = 42 Hz to the other set of H_f and $^4J(^1H^{199}Hg)$ = 24 Hz to H_d were partially obscured by the width of the central peaks corresponding to $^{200/201}Hg$ complexes. Preparation of this sample directly from **7** provided an essentially identical

(21) Åkesson, R.; Sandström, M.; Stålhandske, C.; Persson, I. *Acta Chem. Scand.* **1991**, *45*, 165.
(22) Schomaker, V.; Trueblood, K. N. *Acta Crystallogr.* **1968**, *B24*, 63.
(23) (a) Garoufis, A.; Perlepes, S. P.; Froystein, N. A.; Sletten, J.; Hadjiliadis, N. *Polyhedron* **1996**, *15*, 1035. (b) Canty, A. J.; Minchin, N. J.; Skelton, B. W.; White, A. H. *J. Chem. Soc., Dalton Trans.* **1986**, 2201. (c) Persson, I.; Sandstrom, M.; Goggin, P. L.; Mosset, A. *J. Chem. Soc., Dalton Trans.* **1985**, 1597. (d) Bach, R. D.; Vardhan, H. B.; Maqsudur-Rahman, A. F. M.; Oliver, J. P. *Organometallics* **1985**, *4*, 846. (e) Canty, A. J.; Raston, C. L.; Skelton, B. W.; White, A. H. *J. Chem. Soc., Dalton Trans.* **1982**, 15. (f) Canty, A. J.; Chaichit, N.; Gatehouse, B. M.; George, E. E.; Hayhurst, G. *Inorg. Chem.* **1981**, *20*, 2414. (g) Bell, N. A.; Goldstein, M.; Jones, T.; Nowell, I. W. *Acta Crystallogr.* **1980**, *B36*, 710. (h) Kadooka, M. M.; Hilti, E.; Warner, L. G.; Seff, K. *Inorg. Chem.* **1976**, *15*, 1186.

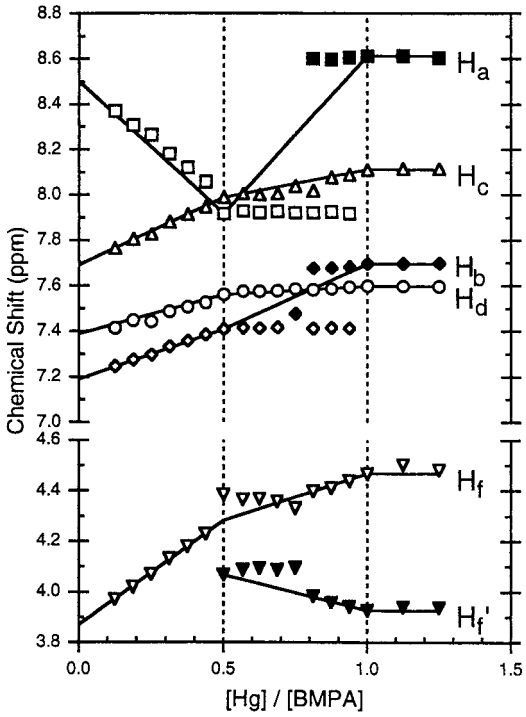

Figure 4. Chemical shifts of protons of BMPA as a function of the nominal $Hg(ClO_4)_2$-to-BMPA ratio in CD_3CN at 20 °C. The concentration of $Hg(ClO_4)_2$ was fixed at 2 mM. The lines represent the chemical shifts expected if interconversion of free ligand, **1**, and **7** were governed by equilibria 1, 2, and 4. Equilibria 2 and 3 are assumed to be highly favorable with $K_2 > K_3 \gg K_1$. Filled symbols are used to indicate that two distinct resonances could be detected for certain protons at metal-to-ligand ratios above 0.5.

spectrum if examined immediately upon dissolution, but a slight excess of metal was required to restore proton−mercury coupling in older samples. Three-bond coupling constants as large as 30 Hz have been reported for the histidine δ- and ϵ-protons of mercury-substituted proteins, and couplings exceeding 50 Hz have only been reported for one other nitrogen coordination compound of Hg(II).[7e] Furthermore, aside from the complexes of TMPA that we recently reported, we are aware of only one other synthetic complex of Hg(II) involving exclusively nitrogen donors for which $^3J(^1H^{199}Hg)$ have been observed near room temperature.[7c] The large difference in ^{199}-Hg coupling to the two methylene protons described here is also of relevance to the development of a Karplus-type relationship for the magnitudes of $^3J(^1H^{199}Hg)$. At metal-to-ligand ratios approaching 2.0, the satellite peaks broadened while the main resonances remained sharp, suggesting ligand exchange with excess metal was becoming significant on the NMR time scale.

Further insight into coordination phenomena was obtained by examining samples containing 2 mM Hg(II) at −40 °C. Except for small temperature effects on the proton chemical shifts, the spectra were identical to those taken at 20 °C below 0.5 equiv of Hg(II). Importantly, the lower temperature reduced exchange broadening at [Hg(II)]/[BMPA] ≈ 0.5 that had obscured mercury−proton coupling. A comparable sample prepared directly from **1** had nearly identical chemical shifts but required addition of approximately 5% excess metal to optimize heteronuclear coupling (Figure S6 (Supporting Information)). Under these conditions, one set of sharp pyridyl resonances were observed with $^3J(^1H^{199}Hg) = 20$ Hz for H_a. In contrast, the methylene protons were detected as two doublets of doublets of approximately equal area. Analysis of heteronuclear coupling satellites revealed $^3J(^1H^{199}Hg) = 69$ and 72 Hz for the two sets of methylene protons (Figure 3). The intensities of the satellite peaks relative to the main portion of the multiplets were consistent with coupling to all methylene protons. Between the [Hg]/[BMPA] mole ratios of 0.5 and 1.0, all the resonances associated with the species prevalent at these two extremes were observed, although with less extensive heteronuclear coupling. In the presence of more than 1 equiv of Hg(II), only a single, strongly heteronuclear-coupled ligand environment was observed, as in the 20 °C spectra.

Increasing the total [Hg(II)] to 100 mM produced significant changes in NMR behavior (Figure S7 (Supporting Information)). In contrast to the approximately linear dependence of chemical shift on [Hg]/[BMPA] observed between 0 and 0.5 equiv of Hg(II) with 2 mM $Hg(ClO_4)_2$, significant deviations from linearity were observed that were most notable for H_a and H_d. The methylene resonance became broadened above 0.5 equiv of Hg(II) but never resolved into two peaks at higher mole ratios. Further increases in the metal-to-ligand ratio caused the chemical shifts of all the pyridyl resonances to move toward the limits observed for the pyridyl resonances in the 2 mM $Hg(ClO_4)_2$ system at or above [Hg]/[BMPA] = 1.0. However, achieving these limits required slightly higher mole ratios. We were unable to detect heteronuclear coupling between ligand protons and the metal center in these high-[Hg(II)] samples.

Although full analysis of the correlation between the solution-state NMR spectra and the solid-state structures is reserved for the Discussion, the spectra described above support formation of cations of Hg(II) and BMPA in acetonitrile solution with stoichiometries of 1:2 and 1:1 as found in complexes **1** and **7**. The four linked equilibria (1)−(4) provide a plausible mechanistic framework.

$$Hg^{2+} + BMPA \rightleftharpoons [Hg(BMPA)]^{2+} \quad (1)$$

$$[Hg(BMPA)]^{2+} + BMPA \rightleftharpoons [Hg(BMPA)_2]^{2+} \quad (2)$$

$$[Hg(BMPA)_2]^{2+} + BMPA \rightleftharpoons [Hg(BMPA)_3]^{2+} \quad (3)$$

$$[Hg(BMPA)_2]^{2+} + Hg^{2+} \rightleftharpoons 2[Hg(BMPA)]^{2+} \quad (4)$$

The net equilibrium constant for formation of $[Hg(BMPA)_2]^{2+}$ has to be much larger than that for formation of $[Hg(BMPA)]^{2+}$ to explain the preference for formation of $[Hg(BMPA)_2]^{2+}$ at low metal-to-ligand ratios. Reaction 3 roughly describes the rapid exchange between free and bound ligands at [Hg]/[BMPA] < 0.5. It is known that mercury(II) can form complexes with as many as eight nitrogen donors, as in $Hg(TMPA)_2^{2+}$,[8] and that BMPA can bond to metals as both a bidentate and a tridentate ligand, as in $Cu(BMPA)_2^{2+}$.[10] Thus, $[Hg(BMPA)_3]^{2+}$ may be a six-coordinate complex in which all three ligands are bidentate or possibly a seven-, an eight-, or even a nine-coordinate complex.

This mechanistic scheme is consistent with the observed trends in chemical shift. If free ligand and $[Hg(BMPA)_2]^{2+}$ were the only BMPA-containing species in solution at metal-to-ligand ratios below 0.5, the chemical shifts of the exchange-averaged resonances would be given by expression 5, in which

$$\delta_{obs} = P_{free}\delta_{free} + (1 - P_{free} - P_{1:1})\delta_{1:2} \quad (5)$$

the weighted average of the chemical shifts of the species present in solution is δ_{obs}, δ_{free} and $\delta_{1:2}$ are the chemical shifts, and

P_{free} and $P_{1:2}$ [$=0.5(1 - P_{free} - P_{1:1})$] are the mole fractions of **3** and **1**, respectively. The chemical shifts would be expected to have a linear dependence on the mole ratio in the region 0−0.5 as shown by the lines in Figure 4 since equilibrium 2 lies far to the right. Large deviations above the lines, particularly at high concentrations, suggest formation of another BMPA-containing species by an associative process. The lines in Figure 4 are continued in the mole ratio region between 0.5 and 1 on the basis of an expression similar to (5) with terms for $[Hg(BMPA)_2]^{2+}$ and $[Hg(BMPA)]^{2+}$ and then depict the observed mole ratio independence. Although residual broadening precludes determination of the equilibrium constants by these methods, the ligand chemical shift differences between $[Hg(BMPA)_2]^{2+}$ and $[Hg(BMPA)]^{2+}$ place the rate of ligand exchange between 192/s (H_b) and 124/s (H_e) under these conditions when [Hg]/[BMPA] is greater than 0.75.

Discussion

Stability constants $\beta_1 = [M(BMPA)]/[M][BMPA]$ and $\beta_2 = [M(BMPA)_2]/[M][BMPA]^2$ have been reported for BMPA with a variety of divalent metal ion nitrate salts in aqueous solution.[15] Mercury(II) had the largest reported value of $\log \beta_2 = 22.25$. The perchorate salt is expected to have a similar value for $\log \beta_2$ in acetonitrile. Seven complexes of type $[M(BMPA)_2]^{2+}$ have been structurally characterized previously.[10,12] Although β_1 was not reported for Hg(II), for eight other metals $\beta_2 \gg \beta_1$ as observed here. A wide variety of complexes of the type $[M(BMPA)]^{n+}$ are known with various other ligands completing the coordination sphere of the metal.

The uncertainties introduced by motional averaging in solution and structural perturbations imposed by packing constraints in the solid require that correlations between solid-state structures and solution-state NMR properties always be made cautiously.[24] Strict preservation of the structures of **1** and **7** in solution would be predicted to give rise to individual resonances for every ligand proton, barring any coincidences in chemical shifts. However, chemical-shift-inequivalent protons are detected in solution NMR only when $k_{ex} < \pi(\Delta\nu)/\sqrt{2}$, where $\Delta\nu$ is the difference in hertz between different exchanging proton environments. Since small structural differences between methylpyridyl groups are unlikely to be preserved in a less vibrationally constrained environment, **7** could be anticipated to have C_s symmetry in solution. Similarly, **1** would have C_2 symmetry. Evidence for formation of cations related to **1** and **7** is provided by consideration of a combination of dynamic motion, symmetry, and heteronuclear coupling arguments.

Acetonitrile solutions containing a nominal 1:2 metal-to-ligand ratio had one peak for each 2-methylpyridyl proton. The $J(^1H^{199}Hg)$ satellites for H_a, H_f, and $H_{f'}$ observed at −40 °C were approximately one-fifth the size of the main resonance. On the basis of available precedent for coordination compounds of Hg(II)[7] and alkylmercurials,[6] the large magnitudes of these coupling constants suggest they arise through three-bond coupling rather than longer range interactions. This implies that bonding interactions are maintained between Hg(II) and all six nitrogens on the time scale of the NMR measurements. The nine regular polyhedral forms for a bis-tridentate chelate are shown in Figure 5. Repulsion-energy calculations have predicted isomers **2**, **4**, and **6** to be associated with potential energy minima,[25] but calculations with updated methodologies have not been identified. The solution-state NMR evidence indicates the meridional complex **6** does not contribute significantly to the solution structure at −40 °C because inversion at the amine nitrogen would interconvert the H_{fa} and H_{fb} environments. The trans-facial complex **4** and trigonal prism **5** are independently consistent with the NMR data for the 1:2 metal-to-ligand complex. However, rapid interconversion among complexes **1**−**5** without bond cleavage provides a racemic mixture which would also be consistent with the solution NMR. Isolation of **1** from acetonitrile solution implies it is part of the equilibrium mixture. Importantly, the two methylene resonances were associated with $^3J(^1H^{199}Hg) \approx 70$ Hz satellites. Geminal methylene protons in the crystallographic structure had average $Hg-N_{am}-C_f-H_f$ dihedral angles of −81(3) and 162(2)°. A normal Karplus-type relationship for ^3J would predict weak coupling for torsion angles close to 90° and large coupling for torsion angles approaching 0 or 180°. Near equivalence of the observed $^3J(^1H^{199}Hg)$ suggests a dynamic process provides comparable average dihedral angles for all the methylene protons.

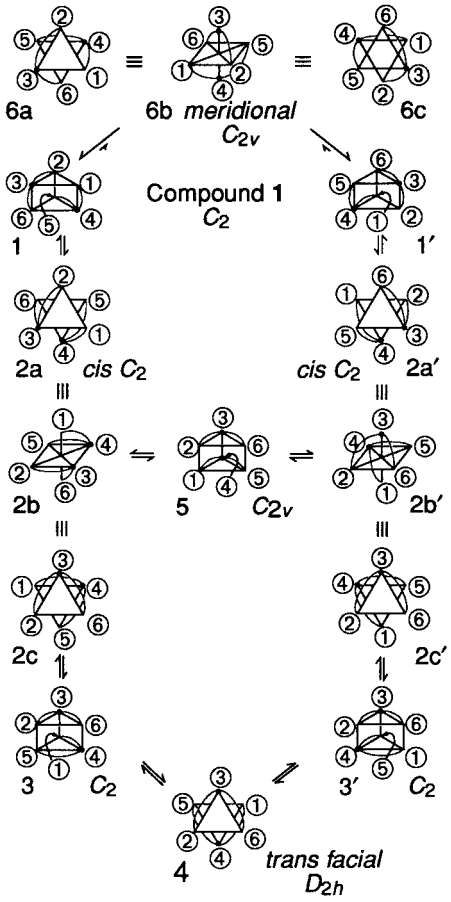

Figure 5. Proposed rearrangement mechanism without bond cleavage for isomeric forms of bis-tridentate chelates.

Rearrangement mechanisms have been proposed for octahedral complexes involving monodentate, mono-bidentate,[26] bis-bidentate,[27] tris-bidentate,[28−30] and hexadentate[31] ligands. A multitwist mechanism for the rearrangements of bis-tridentates

(24) Davies, J. A.; Dutremez, S. *Coord. Chem. Rev.* **1992**, *114*, 201.
(25) Favas, M. C.; Kepert, D. L. *J. Chem. Soc., Dalton Trans.* **1978**, 793.
(26) For example: (a) Johnson, B. F. G.; Rodger, A. *Inorg. Chem.* **1989**, *28*, 1003. (b) Ismail, A. A.; Sauriol, F.; Butler, I. S. *Inorg. Chem.* **1989**, *28*, 1007.
(27) Kost, D.; Kalikhman, I.; Raban, M. *J. Am. Chem. Soc.* **1995**, *117*, 11512.
(28) Bailar, J. C., Jr. *J. Inorg. Nucl. Chem.* **1958**, *8*, 165.
(29) Ray, P. C.; Dutt, N. K. *Indian Chem. Soc.* **1943**, *20*, 81.
(30) Rodger, A.; Johnson, B. F. G. *Inorg. Chem.* **1988**, *27*, 3061.

is proposed in Figure 5. The mechanism is patterned after that described by Rodger and Johnson[30] based on their semiquantitative comparison of the Bailar twist[28] and Ray−Dutt[29] twist for racemization of tris-bidentate complexes. Their work suggests that the energy differences between the Bailar twist and Ray−Dutt twist are minimized for trigonal prismatic structures in which all M−L distances are equal, as is the case in **1**. The multitwist mechanism can be considered a combination of both the Bailar and Ray-Dutt twists in that it involves only rotations about pseudo-C_3 axes of the pseudooctahedral or pseudo trigonal prismatic core of the ligating atoms, but it involves twists about more than one pseudo-C_3 axis. The NMR evidence is inconsistent with the meridional species **6** as described above. Significantly, the crystal structure of **7** suggests meridional coordination of BMPA to Hg(II) would involve significant differences in the Hg−N_{amine} and Hg−$N_{pyridyl}$ bond lengths, which would lead to very high energy transition states.

Examination of the crystallographic data reported for complexes of type $[M(BMPA)_2]^{2+}$ and related systems supports the plausibility of the multistep twist mechanism consistent with the solution-state NMR. The crystal structure of $[Hg(BMPA)_2]^{2+}$ corresponds to the racemic trigonal prismatic structures **1** and **1′** of Figure 1 (**1′** is pictured). The Mn(II), Cd(II), and Zn(II) (form 1) structures with crystallographic C_2 symmetry share this trigonal prismatic geometry.[12a] The complexes with Zn(II) (form 2)[12a] and Cu(II)[10] located at crystallographic inversion centers have achiral structure **4**, molecular symmetry approximately D_{2h}. The pseudooctahedral cis-facial Fe(II) complex, also located at a crystallographic C_2 axis,has structure **2**. It is interesting to note that only the Fe(II) structure is cis-facial, as the crystal field stabilization energy of the low-spin d^6 electron configuration may be required to maintain this isomeric form. The eclipsed trigonal prism **5** is precedented by the structure of (tetrakis(2-pyridylmethyl)ethylenediamine)-iron(II).[30] The ethylenediamine bridge requires the N_{amine} atoms to be cis in an octahedral complex and eclipsed in a trigonal prismatic complex. Comparisons of structures corresponding to selected conformations (Figure S8 (Supporting Information)) suggest these interconversions involve intraligand $N_{pyridyl}$-Hg−$N_{pyridyl}$ angles ranging from 130 to nearly 90° but limited changes in bond lengths consistent with relatively low energy transition states. In summary, the data presented and the structures of known complexes are consistent with $[Hg(BMPA)_2]^{2+}$ existing in solution as a mixture of two achiral species and three sets of enantiomeric pairs. These species have either trigonal prismatic or facial octahedral geometries. Compound **1** corresponds to one of the enantiomeric pairs.

Exchange of ligand between **1** and **7** occurred at an intermediate rate relative to the NMR time scale at 20 °C in the 0.5 < [Hg]/[BMPA] < 1.0 range, leading to considerable peak broadening. Cooling to −40 °C permitted slow exchange conditions to be approached. Although associative exchange processes were documented for ligand exchange between $[Hg(TMPA)_2]^{2+}$ and $[Hg(TMPA)]^{2+}$ under similar conditions, in the BMPA titration multinuclear species were not evidenced by deviations in predicted chemical shift trends or detection of additional resonances. The inability to detect multinuclear complexes of BMPA does not preclude their existence but does indicate they must be less stable than related multinuclear complexes of TMPA.

The proton NMR spectra of solutions containing a 1:1 metal-to-ligand ratio complement the spectra associated with $[Hg(BMPA)_2]^{2+}$ since most protons are deshielded with respect to free ligand and $[Hg(BMPA)_2]^{2+}$. The doublet of doublets associated with two methylene protons ($H_{f'}$) is the only exception. Detection of a single set of pyridyl resonances and two sets of methylene resonances is consistent with a structure of C_s symmetry which does not undergo inversion at the amine nitrogen on the NMR time scale. Extensive ^{199}Hg coupling to the ligand protons implies that all three nitrogens are bound to the metal. Coupling to the pyridyl protons includes $^3J(^1H^{199}Hg) = 46$ Hz for H_a and $^4J(^1H^{199}Hg) = 24$ Hz to H_d which are significantly larger than those observed for $[Hg(BMPA)_2]^{2+}$. Since the Hg−$N_{pyridyl}$−C_a−H_a dihedral angles in **1** and **7** are very close to 0° in the solid state (except for ring 3 in **1**), the solution dynamics of $[Hg(BMPA)_2]^{2+}$ apparently provide an average dihedral angle closer to 90°. Alternatively, there may be additional correlations between $^3J(^1H^{199}Hg)$ and either Hg−$N_{pyridyl}$ bond lengths or the mercury coordination number which need to be resolved through solid-state NMR studies. The $^3J(^1H^{199}Hg)$ of 42 and 80 Hz observed for separate pairs of methylene protons and their larger $\Delta\nu$ also suggest the 1:1 complex has limited dynamics on the NMR time scale. These values bracket the 70 Hz coupling observed in solutions containing a nominal 1:2 metal-to-ligand ratio. Significantly, the −91(10) and 152(10)° average dihedral angles observed for C_s-related protons in **7** would be expected to exhibit a large difference in coupling constant based on a Karplus-type relationship. These data support a cation structure related to **7** in solution, although no direct evidence for the coordination of an equatorial acetonitrile was possible in this experiment or observed in methanol-d_3. Furthermore, acetonitrile may replace the perchlorates involved in close contacts in the solid state.

Conclusion

We have demonstrated that analysis of the equilibria between Hg(II) and a tridentate ligand is facilitated by detection of $J(^1H^{199}Hg)$. The magnitudes of $^3J(^1H^{199}Hg)$ observed here are up to 2 times larger than those of any previous solution studies of mercury coordination compounds involving ligands containing exclusively nitrogen donors.[7a,c] Additional evidence supporting development of a Karplus-type relationship for the magnitudes $^3J(^1H^{199}Hg)$ is presented. Future solid-state NMR studies of crystallographically characterized complexes should reveal dependence on additional factors such as bond length and coordination number. Comparisons of the solution-state ^{199}Hg chemical shifts of **1**, **7**, and related complexes to their isotropic solid-state chemical shifts will also permit the tremendous chemical shift dispersion of ^{199}Hg to probe the similarity of solution- and solid-state structures more directly.

Heteronuclear coupling is not routinely observed between Hg and small organic ligands in solution, even with multidentate ligands. This study demonstrates that, in addition to optimization of solvent, concentration, and temperature, minor adjustments in the metal-to-ligand stoichiometry of small complexes may be necessary to correlate solution trends in $^1H^{199}Hg$ coupling constants with structural features. These adjustments permit spectroscopically detectable exchange to be suppressed. Fortunately, the steric bulk of macroscopic ligands provides an intrinsic deterrent to exchange difficulties. Additional investigations of the mercury coordination chemistry of multidentate ligands whose interactions with physiologically relevant metal ions have been extensively examined will provide valuable resources for the development of ^{199}Hg NMR as a metallobioprobe.

(31) McCusker, J. K.; Rheingold, A. L.; Hendrickson, D. A. *Inorg. Chem.* **1996**, *35*, 2100.

Acknowledgment. This research was supported by the Thomas F. and Kate Miller Jeffress Memorial Trust and by the donors of the Petroleum Research Fund, administered by the American Chemical Society. The NSF-ILI program provided funding for the Bucknell University X-ray diffractometer. R.J.B. acknowledges the DoD-ONR instrumentation program for funds to upgrade the diffractometer and the NIH-MBRS program for funds to maintain the diffractometer.

Supporting Information Available: Figures S1−S10, showing thermal ellipsoid plots, crystal packing diagrams, additional NMR data, and infrared spectra (10 pages). Two X-ray crystallographic files, in CIF format, are available on the Internet only. Ordering and access information is given on any current masthead page.

IC971499+